Predicting the conformational states of cyclic tetrapeptides

ARTICLE *in* BIOPOLYMERS · JULY 2003

Impact Factor: 2.39 · DOI: 10.1002/bip.10339 · Source: PubMed

Nicolas Loiseau[1,2]
Jean-Marie Gomis[3]
Jérôme Santolini[2]
Marcel Delaforge[1,4]
François André[1,2]

[1] *CNRS-URA 2096, Protéines Membranaires Transductrices d'Énergie, DBJC, CEA–Saclay, 91191 Gif-sur-Yvette cedex, France*

[2] *Service de Bioénergétique, Département de Biologie Joliot-Curie CEA–Saclay, F-91191 Gif-sur-Yvette cedex, France*

[3] *Service des Molécules Marquées et Chimie Bioorganique, Département de Biologie Joliot-Curie, CEA–Saclay, F-91191 Gif-sur-Yvette cedex, France*

[4] *LEMM, Service de Pharmacologie et d'Immunologie, Département de Recherche Médicale, CEA–Saclay, F-91191 Gif-sur-Yvette cedex, France*

Predicting the Conformational States of Cyclic Tetrapeptides

Received 25 July 2002; accepted 4 November 2002

Abstract: *Biologically active cyclic tetrapeptides, usually found among fungi metabolites, exhibit phytotoxic or cytostatic activities that are likely to be governed by specific conformations adopted in solution. For conformational studies and drug design, there is a strong interest in using fast and reliable methods to determine correctly the conformational population of cyclotetrapeptides. We show here that standard molecular mechanics computational approach gives satisfactory results. The method was validated step by step by experimental data either obtained after synthesis and NMR analysis, or found in the literature. The cyclo(Gly)$_4$, cyclo(Ala)$_4$, cyclo(Sar)$_4$, and cyclo(SarGly)$_2$ peptides were used to evaluate the prediction of the peptide backbone conformation, and the*

Correspondence to: François André; email: andre@dsvidf.cea.fr

Contract grant sponsor: CNRS, Ministère de l'Éducation Nationale (MEN), and Ministère de l'Aménagement du Territoire et de l'Environnement (MATE)

Contract grant number: PCV97-185 (CNRS), ACC-SV5 No. 9505221 (MEN), and AC009E (MATE)

This article includes supplementary material available via the Internet at http://www.interscience.wiley.com/jpages/0006-3525/suppmat/2003/69/v69.3.363.html

Biopolymers, Vol. 69, 363–385 (2003)

detailed conformational analysis of tentoxin, a natural phytotoxic cyclotetrapeptide in which N-alkylated peptide bonds alternate with regular secondary ones, was used to validate the computation of conformers proportions. From the knowledge of an initial cyclic primary structure and of the D *or* L *configuration of the amino acids, we show that it is possible to determine the exact orientation of carbonyl groups and to predict the nature of conformers present in solution. The proportion of each conformer can be inferred from a statistical thermodynamics approach by using the potential energy values of each conformer, computed by molecular mechanics methods with the TRIPOS force field, which allowed us to account for the solvent. The solvent contribution was processed by two different methods according to the nature of the interactions: whether through the dielectric constant introduced in the electrostatic potential, when interaction with solute molecules are weak or negligible, or through the computation of free energy of solvation using the algorithm SILVERWARE© for solvents explicitly interacting with the solute. When applied to tentoxin, this conformational analysis yielded results in very good agreement with the experimental data reported by Pinet et al. (*Biopolymers*, 1995, Vol. 36, pp. 135–152), on both the nature of existing conformers and their relative proportions, whatever the nature of the considered solvent.* © 2003 Wiley Periodicals, Inc. Biopolymers 69: 363–385, 2003

Keywords: *conformational analysis of cyclotetrapeptides; cyclic peptides; proton NMR spectroscopy; molecular mechanics; tentoxin*

INTRODUCTION

The selectivity, metabolic stability, and biological potency of peptides can be improved by introduction of severe conformational constraints such as cyclization. One advantage of the cyclic form is that the peptide can assume only a limited number of distinct conformations. One problem, however, is to assess the structural features and the proportions of each conformer, especially when conformational exchange occurs and is fast on the NMR time scale. In most bioactive cyclopeptides known so far, individual conformers cannot be isolated as stable compounds and therefore cannot be tested separately for biological activity. Thus, while the cyclic peptide has been designed to assume few conformations, it is yet difficult to identify which of these are able to bind their receptor, and hence to establish the structural and dynamic characteristics that are crucial for the biological activity. In a drug lead discovery perspective, molecular modeling routines able to predict correctly the various structures that are interconverting in cyclic peptides, and to work out their relative proportions, are of obvious interest.

We are interested in developing the chemistry of a particular class of cyclic peptides, the cyclotetrapeptides. Many biologically active cyclopeptides indeed have been described, but only a few naturally occurring cyclotetrapeptides have been fully characterized. These usually demonstrate strong and various interesting activities, such as host-specific or species-specific phytotoxic activities, or cytostatic effects. In Table I, the primary structure of known cyclotetrapeptides are displayed along with their biological activities. Specific structural features such as D-amino acid residues, secondary amide bonds (including proline), dehydro-amino acid residues, or exotic amino acid residues are often found in natural fungal cyclopeptide products, and their presence generally controls the peptide ring conformation. Tentoxin (**1**)[1,2] and AM-toxin I (**2**),[3,4] characterized by three L-amino acids and one α,β-dehydrogenated residue (Figure 1), exhibit host or non host-specific phytotoxic activities. Cyl-1 (**3**),[5] Cyl-2 (**4**),[6,7] and HC-toxin (**5**),[8–11] which are also phytotoxic peptides, possess a D-residue instead of the dehydro-residue, and are marked by the presence of a novel amino acid residue, L-Aoe. The presence of L-Aoe and the analogous residue L-Aod also characterizes the next group of cyclotetrapeptides in Table I comprising chlamydocin (**6**),[12–14] trapoxin A (**7**), trapoxin B (identical to trapoxin A with a D-Pro residue in place of the D-Pip residue),[15] apicidin (**8**), apicidin A [identical to Apicidin with L-Trp in place of L-Trp(N-OMe)],[16] and WF-3161 (**9**).[17] All these peptides present cytotoxic or cytostatic activities and possess one D-amino acid and three L-amino acids, including L-Aoe or L-Aod. In this tentative classification, a last group of cyclopeptides can be distinguished, including fenestin A (**10**),[18] cyclo(L-Pro–L-Val)$_2$ (**11**),[19] cyclo(L-Pro–L-Leu)$_2$ (**12**), cyclo(L-Pro–L-Phe)$_2$ (**13**), and cyclo(L-Pro–L-Tyr–L-Pro–L-Val) (**14**),[20] all characterized by four L-amino acids, and exhibiting cytotoxic activities as well.

In most cyclotetrapeptides there occurs a multiconformational equilibrium.[21] The biological activity may depend on a particular conformation or on a group of conformations. Studying the precise relationship that exists between the primary structure of the cyclopeptides and their conformation becomes a mat-

Table I Primary Structures, Biological Activities, and Producing Organism of Natural Cyclic Tetrapeptides

		Primary Structure Shown as cyclo(-1-2-3-4-)						
Entry	Name	1	2	3	4	Activity	Organism	Ref.
1	Tentoxin	L-*N*MeAla	L-Leu	*N*MeΔ(Z)Phe[a]	Gly	Phytotoxic	Fungus *Alternaria alternata*	1,2
2	AM-toxin I	L-Ala	L-Hmb[b]	L-Amp[c]	ΔAla[d]	Phytotoxic	Fungus *Alternaria mali*	3,4
3	Cyl-1	L-Pro	L-Aoe[e]	D-Tyr(OMe)	L-Ile	Phytotoxic	Fungus *Cylindrocladium scoparium*	5
4	Cyl-2	L-Pip[f]	L-Aoe	D-Tyr(OMe)	L-Ile	Phytotoxic	Idem	6,7
5	HC-toxin	D-Pro	L-Ala	D-Ala	L-Aoe	Phytotoxic (2nd activity cytotoxic)	Fungus *Cochliobolus carbonum*	8–11 (46,47)
6	Chlamydocin	Aib	L-Phe	D-Pro	L-Aoe	Cytostatic	Fungus *Diheterosporia clamydosporia*	12–14
7	Trapoxin A	L-Phe	L-Phe	D-Pip	L-Aoe	Cytotoxic	Fungus *Helicoma ambiens*	15
8	Apicidin	L-Trp(N-OMe)	L-Ile	D-Pip	L-Aod[h]	Histone deacetylase inhibitor	Fungus (various *Fusarium* species)	16
9	WF-3161	D-Phe	L-Leu	L-Pip	L-Aoe	Cytotoxic	Fungus *Petriella guttulata*	17
10	Fenestin A	L-Pro	L-Pro	L-Leu	L-Ile	NA[i]	Marine sponge *Leucophoelus fenestra*	18
11	cyclo(Pro–Val)$_2$	L-Pro	L-Val	L-Pro	L-Val	Cytotoxic	Tunicate *Cystodytes delle chiajei*	19
12	cyclo(Pro–Leu)$_2$	L-Pro	L-Leu	L-Pro	L-Leu	Cytotoxic	Idem	19
13	cyclo(Pro–Phe)$_2$	L-Pro	L-Phe	L-Pro	L-Phe	Cytotoxic	Idem	19
14	cyclo(Pro–Tyr–Pro–Val)	L-Pro	L-Tyr	L-Pro	L-Val	Tyrosinase inhibitor	Bacterium *Lactobacillus helveticus*	20

[a] *N*-methyl-Z-dehydrophenylalanine.
[b] Hmb, 2-hydroxy-3-methylbutanoic acid.
[c] Amp, 2-amino-5-(*p*-methoxyphenyl) pentanoic acid.
[d] Dehydroalanine.
[e] Aoe, 2-amino-8-oxo-9,10-epoxydecanoic acid.
[f] Pip, pipecolic acid.
[g] Aib, α-aminoisobutyric acid.
[h] Aod, 2-amino-8-oxo-decanoic acid.
[i] NA, none available.

ter of strong interest since the observed biological activity can be credited to a given conformer. So far, too little general rules have been established to describe this relationship, except Kato et al., [22] who put forward few empirical rules that tentatively predict the backbone conformations of cyclic tetrapeptides and tetradepsipeptides, but that suffer from too many exceptions to apply to all primary sequences. What is missing today is a more general method that allows modeling of multiconformational equilibria present in rings homologous to that of cyclotetrapeptides, in order to predict the proportions of the different conformers in solution within a given family (such as TCTC, or *trans–cis–trans–cis* family).

In the present study, we describe a method that allows fast and reliable quantitative predictions of conformer equilibria in cyclotetrapeptides, particularly accurate when implemented with solvation algorithms. We focused on the conformational system of tentoxin, a natural cyclotetrapeptide excreted by a phytopathogenic fungus, which has been shown to possess clearly defined conformations in water,[26] an appealing feature for drug design. Its conformer distribution has been fully characterized by NMR spectroscopy at different temperatures, in various aqueous and organic solvents,[23] making it a good starting theoretical model for such an analysis. Tentoxin is also a lead peptide for studying cyclic tetrapeptides

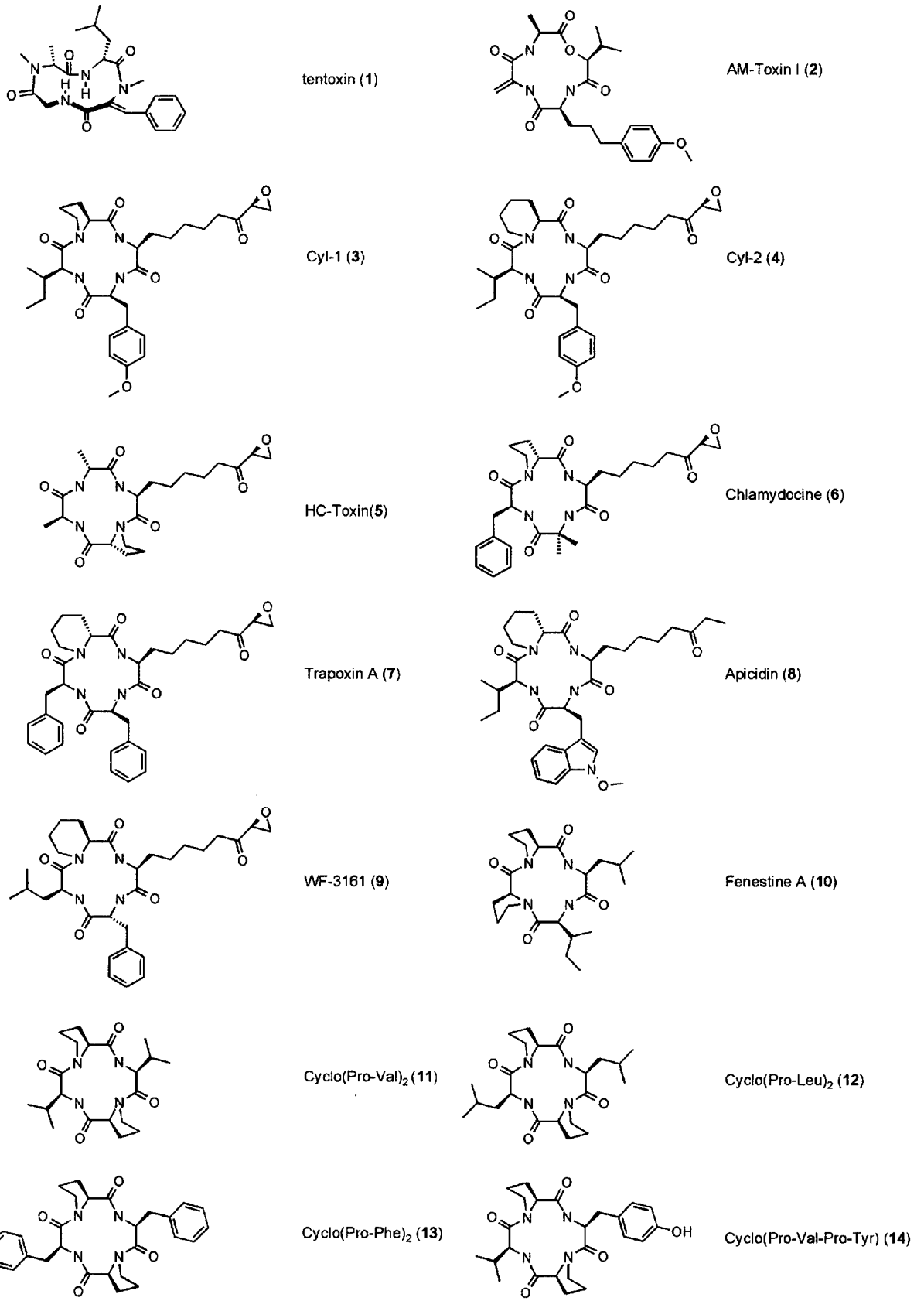

FIGURE 1 Structures of fourteen natural cyclotetrapeptides. Biological activities and producing organisms are reported in Table I.

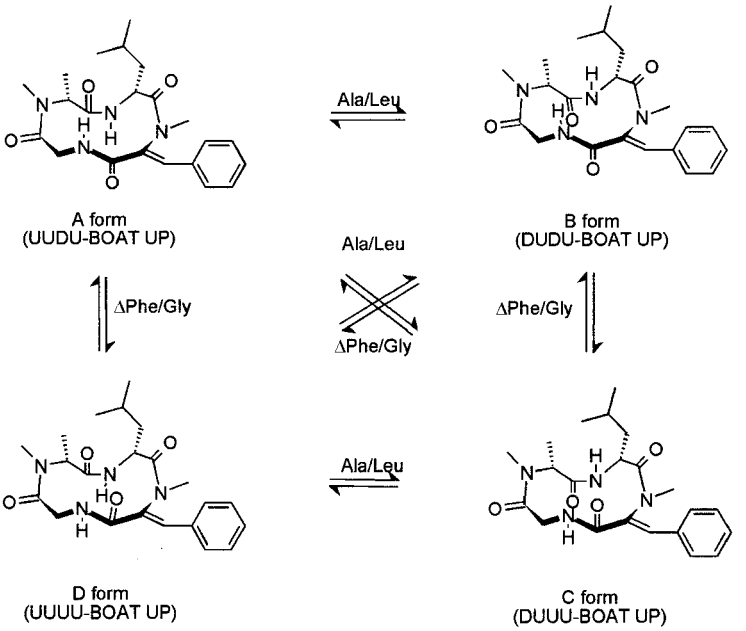

FIGURE 2 Schematic representation of four tentoxin conformations in chemical exchange. The conversion from one conformation to another is done via peptide bond inversion indicated on the arrows.

owing to the fact that the same molecule gathers most of the general features encountered in toxic cyclotetrapeptides: presence of N-alkylated residues, one α,β-dehydro amino acid, one Gly residue, alkyl or aromatic side chains, all the chiral centers being in L configuration. The solution structure of tentoxin was first determined in deuterated chloroform at 300 MHz in 1978 by Rich et al.[24,25] These authors found a single conformation, probably because at room temperature the resonances were averaged by a fast exchange on the NMR time scale. The study published by Pinet et al.[26] in 1995 showed indeed evidence for an equilibrium between four distinct conformers in aqueous solution (depicted in Figure 2), and between the two major forms A and B in deuterated chloroform,[23] in the proportions indicated in Table II. The cyclic structure of the four conformers was confirmed to be alternated *cis–trans* (CT) for N-methylated and non-N-methylated amide bonds, respectively. Within the TCTC conformational family, only the boat-like conformers were detected (referred as to A, B, C, and D by Pinet et al.), if we omit the fact that the D form was not directly observed in ^{1}H-NMR spectra, but deduced from the logical interconverting conformer scheme of Figure 2 that involves the rotation around non-N-methylated peptide bonds.

Table II Experimental Proportions of Tentoxin Conformers According to Temperature and Solvent (NMR Data[26])

Solvent	Temperature	%A	%B	%C	%D
D_2O	−5°C	51	37	8	4
D_2O	85°C	44	39	16	—
$DCCl_3$	−45°C	13	86	—	—

Finally, we explain why only boat-like conformations of the alternate configuration TCTC were observed in solution, whereas other forms could have theoretically been found, and we show how the exact proportions of the conformers can be inferred from molecular mechanics calculations, in various temperature and solvent conditions.

MATERIALS AND METHODS

Conformational Nomenclature

To describe exhaustively the range of cyclotetrapeptide conformations, we assumed the following nomenclature rules.

Primary Structure of Cyclic Peptides. As cyclic peptides do not present N- and C-terminal ends, standard numbering of residue valid for linear peptides cannot hold. We applied instead specific numbering of amino acids in the direction N- to C-edges, starting from the residue whose symbol is a letter of lowest rank in the alphabet. Exotic

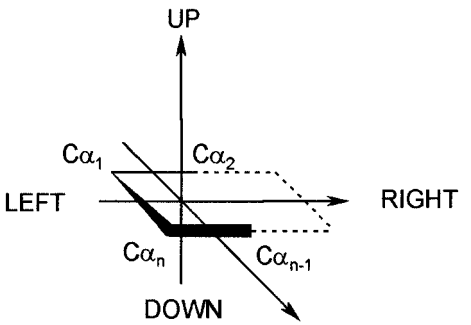

SCHEME 1 Schematic representation of cyclotetrapeptides mean plane and of clockwise orientation of peptide groups.

residues (other than N-methylated amino acids) were ascribed the character Z. For analogues of a lead cyclopeptide, we retained the residue numbering applying to the lead molecule.

Backbone Conformations of Cyclic Peptides A first level of description of cyclopeptide conformations relates to the sequence of *cis* or *trans* peptide bonds. Throughout this report, we consistently identify the conformational sequence by starting by the conformation of the peptide bond connecting the first and the second residue in our numbering. For conformational sequences others than all-*trans* or all-*cis*, letters C and T are used to refer to conformation *cis* and *trans*, respectively (e.g., TCTC).

Imino and Carbonyl Groups Orientation in Cyclic Peptides. A second level of description of cyclopeptide conformations relates to the orientation of peptide carbonyl groups either upward or downward with regard to the mean plane of the ring. The orientation of the ring is identified as shown in Scheme 1: by convention, the average plane of the ring is defined by a mean plane of Cα positions, the residues are arranged clockwise, and the orientation of carbonyl groups from residue 1 to N is sequentially denoted by letter U or D, when carbonyl groups are oriented towards the upper side or towards the lower side of the ring, respectively.

Overall Conformation of Cyclic TCTC Tetrapeptides. An optional convention was adopted to depict in a more figurative-like manner the conformers of TCTC genus in cyclotetrapeptides such as tentoxin. As illustrated in Figure 5, the TCTC backbone conformation presents four families of conformers differing by the overall shape of the ring, that we named respectively BOAT UP, CHAIR LEFT, CHAIR RIGHT, and BOAT DOWN, by analogy to cyclohexane conformations. The orientation of the chair-like and boat-like structures are defined according to the directional axis described in Scheme 1.

With the help of these nomenclature rules, we can describe exactly all the tetracyclopeptide conformers. In particular, the conformers of tentoxin experimentally characterized in aqueous solution by Pinet et al.,[26] designated as A, B, C, and D forms, correspond to UUDU, DUDU, DUUU, and UUUU conformers, respectively, in our nomenclature. These conformers are all BOAT UP in their overall conformation.

Computational Methodology

The geometrical and energetical optimization of the various conformations was carried out using SYBYL 6.5 running on a Silicon Graphics INDY R4400SC workstation. We used the TRIPOS[27] force field because it was primarily parameterized for peptides. Charges computation was achieved using the PULLMAN[28] method with a cutoff of 20 Å in non-solvated systems and 40 Å in solvated systems. Energy minimizations were carried out according to the Powell[29] method using a gradient of 0.05 kcal/(mol · Å). In the following, minimizations in vacuo referred to calculations performed with dielectric constant taken constant and equal to 1, by opposition to minimizations in solvated system. This study was carried out in four steps described below. Two initial steps were performed for the construction of consistent structures, ready to be optimized: optimization in vacuo of a starting conformation TCTC; then optimization in vacuo of all subconformers belonging to the TCTC family (including conformations A, B, C and D of tentoxin), derived from the lead starting TCTC conformation by applying specific constraints. The two last steps concerned building and optimization of the solvated systems of A, B, C and D according to two methods: either by the SCRF[30] method (Self-Consistent Reaction Field) using the dielectric constant of the given environment, or by the DROPLET[31–33]method, based on coating of the solute in several layers of solvent molecules.

Step 1: Building and Optimization of a Basic TCTC Structure In Vacuo. To generate the various conformations found in aqueous solution, a generic alternated TCTC structure of tentoxin ring was built using the drawing interface under SYBYL. This initial structure of peptide conformational sequence TCTC had a significant cyclic bending energy, that a sole energy minimization could not relax satisfactorily. This structure was thus submitted to constrained molecular dynamics in vacuo at 300 K during a time of acquisition of 100 fs with a step of 5 fs and a thermal coupling coefficient of 10 fs. The constraints concerned simply the dihedral angles ω of amide bonds, with values of 0° or 180° to allow for *cis* and *trans* conformations, respectively, with a constraint force on the dihedral angle set to 0.05 kcal · mol^{-1} · deg^{-1} according to a harmonic potential. This molecular dynamics simulation allowed us to find the lowest energy area of the conformational space without changing ring conformation. The constraints were discarded before final minimization. This generic optimized TCTC structure was the starting structure to generate the various subconformations.

Step 2: Building and Optimization of Cyclopeptide Conformations of the TCTC Family. The various subconformations are discriminated by the respective orientation of their carbonyl groups, either upper side - or lower side - directed with respect to the average plane defined by the position of α-carbons in the tetrapeptide ring. To derive these new structures, we carried out a molecular dynamics simulations under constraints that takes into account the whole twelve dihedral angles of the tetrapeptide ring, and not only the dihedral angles ω. These angular constraints were adequate to control the carbonyl orientations and to discriminate the sixteen conformations. Dynamics simulations were realized at 100 K, during 1000 fs with steps of 5 fs. The final energy minimization, achieved to reach the energy minimum of each conformer, was carried out in vacuo without constraints. These minimized structures were then used as starting structures for further energy calculations involving the solvent contribution.

Step 3: Solvation by the SCRF Method. In this basic approach, the solvent contribution was taken into account by adjusting the value of dielectric constant ϵ, according to the nature of the solvent under consideration. The different conformations optimized in vacuo (step 2) were first submitted to constrained molecular dynamics (with ω peptide bond angles as unique constraints to prevent transconformation during calculation) at 100 K during 100 fs with steps of 5 fs to relax the ring, with solvent dielectric constant ϵ. Resulting conformations were lastly energy-minimized without constraints.

Step 4: Solvation by the DROPLET Method. In this approach, the nature of the solvent was taken into account by optimizing a solvated complex of solute and solvent molecules. Using the SILWERWARE©[33,34] solvation algorithm and the DROPLET method, we solvated each conformer by two layers of solvent molecules in the three directions of the space. About three hundred solvent molecules were thus generated surrounding the solute molecule, which is sufficient to obtain a uniform solvation. After a first minimization in vacuo, this solvated system was optimized by constrained molecular dynamics, using ring constraints characterizing each studied conformer (see Supplementary Material, Table S1). The dynamics was carried out at 100 K during 1000 fs with steps of 5 fs and with a thermal coupling of 10 fs. Each form was then energy-minimized under these constraints, with a dielectric constant value set according to the medium. Constraints were then removed for final minimization.

Numerical Processing of Multiconformational Equilibria

A calculation method, based on the JIROUSEK[35] method, was adapted to determine the proportion of *n* conformations in chemical exchange at a given temperature. If we consider an equilibrium between two interconverting species X and Y, with equilibrium constant K_{XY}, the *Boltzmann* relation applies as follows:

$$K_{XY} = \exp[-\Delta G_{XY}/(R.T)] = N_Y/N_X \quad (1)$$

where N_X and N_Y are, respectively, the molar fractions of X and Y compounds, and where, according to the *Gibbs* relation:

$$\Delta G_{XY} = \Delta H_{XY} - T.\Delta S_{XY} \quad (2)$$

where ΔG_{XY} is the free enthalpy variation of the equilibrium, ΔH_{XY} the enthalpy variation, and ΔS_{XY} the entropy variation.

The system studied is a chemical equilibrium between two conformations, at constant pressure and temperature. For each side of the equilibrium, the reference state is the same, from the point of view of molecular mechanics and of thermodynamics. Thus, under fixed conditions of temperature and pressure, we can neglect the entropy variation (ΔS_{XY}), and compare the enthalpy variation (ΔH_{XY}) to the difference in total energy ($E_Y - E_X$) of species X and Y derived from molecular mechanics.[36] This formulation can be generalized to a chemical equilibrium between *n* interconverting conformations. A form *i* in multiple equilibrium with the other $n - 1$ forms fulfills the relation (1) for each equilibrium. Thus

$$K_{i,j} = N_j/N_i = \exp[-(E_j - E_i)/(R.T)] \quad (3)$$

With normalization:

$$\sum_{j=1}^{n} N_j = 1$$

and

$$N_i = 1/(\sum_{j=1}^{n} K_{i,j})$$

The population N_i of the conformational state *i* can be related to the energies derived from molecular mechanics according to:

$$N_i = \exp[-E_i/(R.T)]/(\sum_{j=1}^{n} \exp[-E_j/(R.T)]) \quad (4)$$

RESULTS AND DISCUSSION

Two levels of conformational structuration can be defined in a cyclotetrapeptide: the first one relates to the sequence of peptide bonds conformations (*cis* or *trans*), and the second one defines the orientation of carbonyl groups of the corresponding bonds (relative to the mean plane defined by the tetrapeptide ring).

According to NMR data, tentoxin presents the sequential conformation *trans–cis–trans–cis* for peptide bonds (1,2)—(2,3)—(3,4)—(4,1) respectively. In 1987, Kato[22] proposed five empirical rules to predict the conformation of a cyclic tetrapeptide, on the basis of conformations observed in natural cyclopeptides. These rules provide a way to find the conformational sequence of peptides bonds in delineated situations, but they were mainly derived from NMR data collected in chloroform, and no theoretical arguments supported them. In addition, these rules predict only one conformation for a given cyclotetrapeptide, and do not account for the multiconformation equilibrium that governs most natural cyclic peptides.

Our approach mainly utilizes the conformational analysis as provided by current available computational chemistry tools. Indeed, standard peptide conformational search methods as well as molecular dynamics simulations did not allow the observation of conformational transitions in the tentoxin ring such as the inversion around non-methylated peptide bonds, as quoted by Pinet et al.[26] in 1995. This is due to the ring strain that predominates in small cyclopeptides, whose high-energy barrier cannot be easily overcome by unconstrained molecular dynamics or comprehensive conformational search. As the conformational space of cyclotetrapeptides is severely restricted by peptide bond conformations and by dihedral angles consistent with ring closure, this allows us to be exhaustive in the definition of the backbone of all fundamental conformations, and to generate them either manually or through constrained molecular dynamics simulations. The other structural features of the cyclopeptide (such as the presence of side chains, their nature, and their chirality) can then be introduced to carry out a progressive analysis of the conformation, and in this context, the proportions of the most stable conformers can be easily derived from the Boltzmann relation.

We thus show in the following sections (1) how molecular mechanics provide consistent information to determine the dominant backbone conformation adopted by the cyclopeptide; (2) how to determine, within this preferred backbone conformation, the nature and the proportions of the various subconformers in equilibrium; and (3) how the solvent can influence the proportions of the different substates at the equilibrium.

Backbone Conformation as Determined from Molecular Mechanics Arguments

Definition of Influential Parameters. Numerous factors govern the conformation of cyclopeptides: for example, the nature of amino acids (steric bulk of side chains, L or D configuration), the presence of dehydroamino acid, the presence of N-methylation, the ability to form γ-turns. Predicting the correct conformation is thus difficult without knowing the influence of each of these factors individually. It is, however, possible to discriminate two groups of parameters: those contributing to the ring strain, and those corresponding to nonbonded interactions. The energy associated to the ring strain is the sum of the bond stretching energy, the angle bending energy, the torsional energy, and the out-of-plane bending energy. The energy characterizing the nonbonded interactions comprises the electrostatics and van der Waals interactions, which includes hydrogen bonding, transannular repulsive interactions, and hydrophobic interactions.

To evaluate the relative influence of these two classes of energy parameters, we compared the conformational properties of two model cyclopeptides: cyclo$(Gly)_4$, which was proved to display a TTTT (all-*trans*) conformation,[37,38] and tentoxin, found in the alternating TCTC conformation.[26] The use of cyclo$(Gly)_4$ is a gain in a theoretical approach, since it possesses no side chains, thus allowing us to neglect their influence and to examine independently the influence of ring strain and electrostatic interactions (including in particular intramolecular hydrogen-bond contributions) on the peptide ring. Tentoxin, in turn, offers two important benefits: the presence of a variety of side chains, the presence of N-methylations, and thus the possibility to measure their influence on hydrogen bonds formation.

Influence of Ring Strain. For any cyclotetrapeptide, it is possible to define six conformational sequences of peptide bonds: TTTT, TCTT, TCCT, TCTC, CCCT, and CCCC (all-*cis*). In order to visualize only the ring strain within the tetrapeptide cyclic backbone in the six conformations, we developed the symbolism displayed in Figure 3(panel A), in which the simultaneous deformation of the four NCαC valence angles depicts the ring strain. In such a representation, the side-chain effects, electrostatic contributions, and energy difference between *cis* and *trans* conformations of peptide bonds are not taken into account. It allows us to privilege the planar character of peptide bonds, at the expense of the geometry of Cα atoms. In reality, as shown by the structure of cyclo$(Gly)_4$ displayed in Figure 3B, the molecule compensates for the strain thus generated at the level of Cα atoms by a significant out-of-plane deformation of the *trans* peptide bonds.

Because of this symbolism, the all-*trans* form artificially exhibits $N_iC\alpha_iC'_i$ valence angles equal to 90°

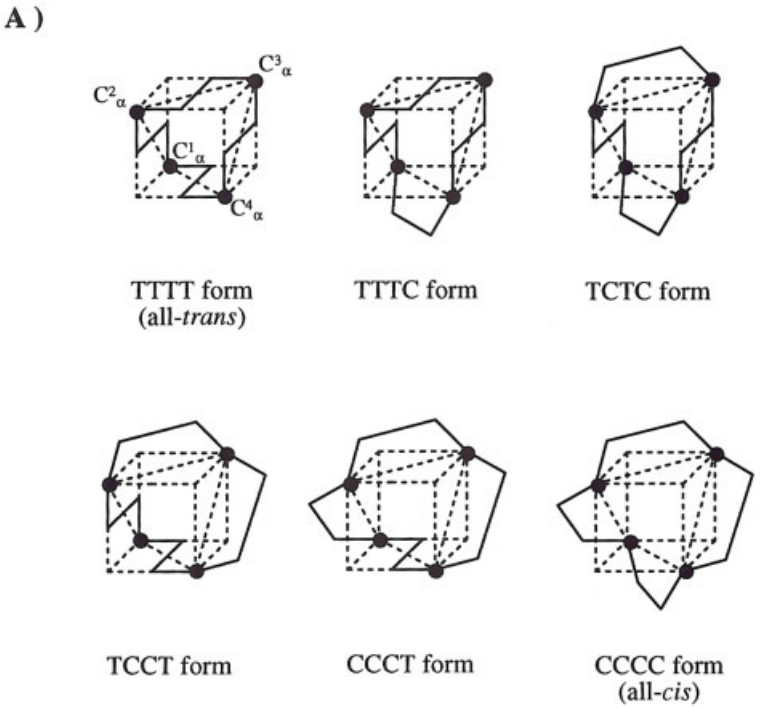

B) Model of cyclo(Gly_4) all-*trans* form.

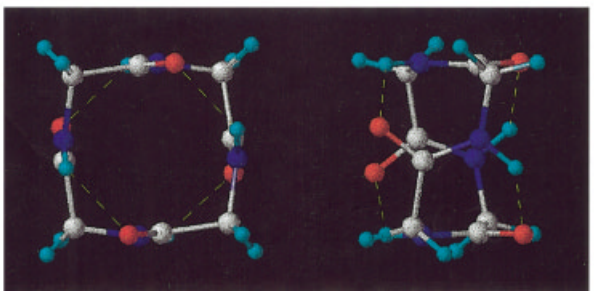

FIGURE 3 Panel A: schematic description of the six conformational states of cyclotetrapeptide backbone. A cyclic tetrapeptide has four α-carbons that can be arranged at opposite corners of a cube. The diagonals of the faces connect two consecutive α-carbons, defining rotational axes of peptide planes. In this representation, NCαC angles are depicted with 90° angles to schematize the Csp3 atoms geometry, when the Cα atom connect two consecutive *trans* peptide bonds. Planarity of peptide bonds is strictly respected by using this cubic formalism, and the ring strain is transferred to Cα atoms by deviation from ideal geometry. Panel B: all-*trans* conformation of cyclo$(Gly)_4$[37, 38] shows that the cyclotetrapeptide backbone redistributes the ring strain over the peptide bonds by out-of-plane bending, so that the Cα atoms valence angles get closer to the Csp3 geometry (109°28′). The real NCαC angle value is found to be equal to 104°16′. This cubic model is used to emphasize the whole deformation induced by the ring strain solely on Cα atoms, for a visual analysis of the ring strain effect on the cyclopeptide conformation.

(which are normally found 104°16′), in order to respect torsion angles ω values at 180° in each peptide bond. Increasing the $N_iC\alpha_iC'_i$ angle values to more than 90° requires the distortion of the other angles, and thus would increase the ring strain. The five other conformational sequences have at least one peptide bond in the *cis* conformation, and the presence of a *cis* bond in the peptide ring allows us to compensate naturally for the angular deformations. In addition, $C\alpha_iC\alpha_{i+1}$ distances are higher in *trans* peptide bonds than in *cis* peptide bonds. Thus, the TCTT, TCCT, and CCCT are subjected to an additional ring strain due to the loss of symmetry, as compared to the TCTC, all-*trans* and all-*cis* forms. Last, the all-*cis*

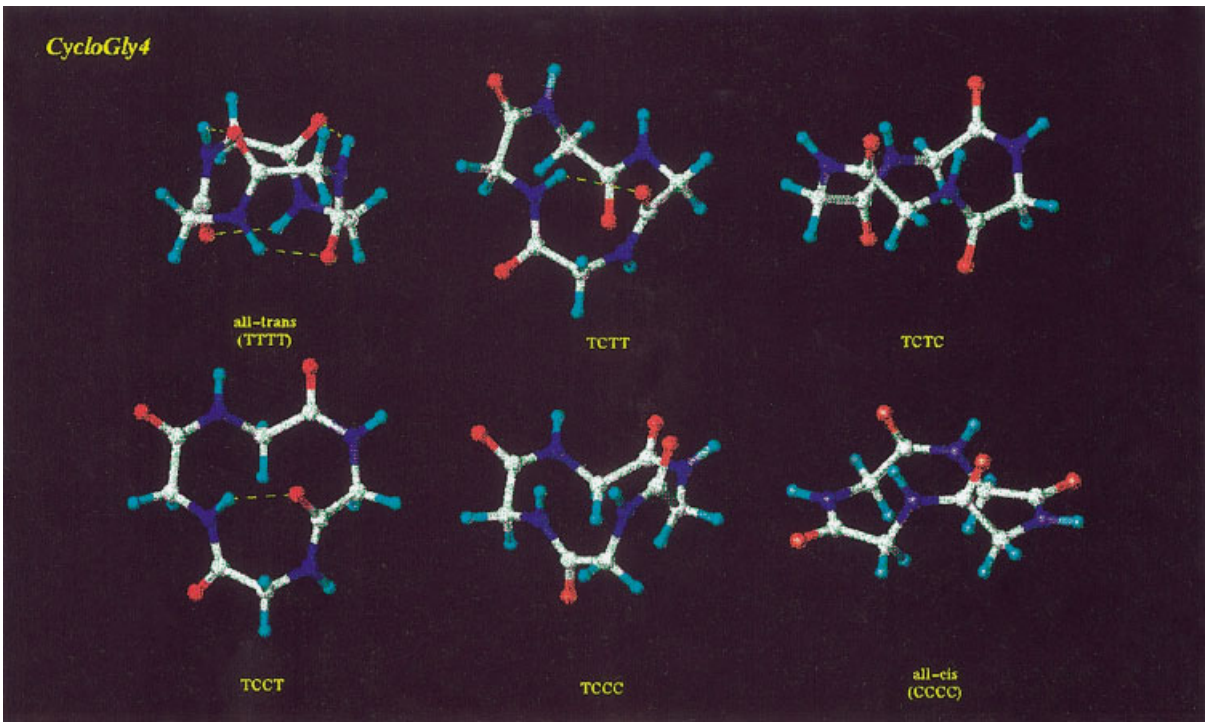

FIGURE 4 Models of the six conformational states in cyclo(Gly)$_4$. Intramolecular hydrogen bonds, represented as yellow dotted lines, were calculated by SYBYL©.

form experiences an additional constraint in ring strain due to the proximity of the Cα's, as a consequence of four shorter Cα_iCα_{i+1} distances. As illustrated in Figure 3, the TCTC form appears to be the most relaxed form, since it allows us to better comply with the Cα sp^3 or sp^2 atom geometry, unlike all the other conformations. The TCTC sequence is thus the most favored conformation among the six possible families. It is less obvious to define a stability order between the five other forms. The essential consequence of this first symbolic approach is that, when applied to tentoxin, it becomes clear that the presence of one dehydro-amino acid disturbs the ring strain, which can be compensated only under the TCTC conformational sequence.

cyclo(Gly)$_4$ Computed Model. Using cyclo(Gly)$_4$ as a model, we generated under SYBYL© the six conformations displayed in Figure 3, using basic constraints on dihedral angles ω. Each form was optimized in vacuo. The results of energy minimization are displayed in Figure 4, where intramolecular hydrogen bonds are represented as yellow dotted lines. The TCCC and all-*cis* conformations showed no intramolecular hydrogen bond (Figure 4) able to stabilize them, in agreement with the fact that they were not favored in the model of Figure 3. TCCT and TCTT conformations present a stabilizing hydrogen bond. The all-*trans* conformation exhibits four hydrogen bonds, which result in a strong stabilization. And the TCTC form, which exhibited the lowest ring strain in Figure 3, does not experience any stabilization by hydrogen bonding. Examination of the various energy terms of cyclo(Gly)$_4$ (Table III) indicates that the all-*trans* form is the most stabilized form, according to total energy value. TCTC and TCTT forms are then found less stabilized, and the three other forms appeared to be the less favored conformations.

From the various energy terms, we can derive a parameter typically representative of the ring strain, defined as the sum of energy terms associated to bond stretch, valence angles, dihedral angles, and improper angles (sum of bonded energy terms, displayed in Table III), and of the terms associated with intramolecular electrostatic interactions (sum of electrostatic energy factors, displayed in Table III), that also account for hydrogen bonding. From the point of view of these two contributions (bonded and electrostatic) in the cyclo(Gly)$_4$ structure, it can be deduced that the order of stabilization is consistent with that deduced from ring strain depicted in Figure 3: the ring strain of the TCTC form is the lowest despite the presence of the two *cis* conformations (that are not favorable) in the peptide ring. From the electrostatic energy point

Table III Energy Terms (in kcal · mol^{-1}) of Various Minimized Forms of cyclo(Gly)$_4$

	TTTT	TCTC	TCTT	CCTT	CCCT	CCCC
Bond stretching energy	0.552	0.730	0.702	0.848	0.988	1.023
Angle bending energy	2.205	4.988	3.558	5.561	8.371	9.415
Torsional energy	8.537	4.988	6.892	6.108	5.175	5.041
Out-of-plane bending energy	2.487	0.124	0.997	0.315	0.103	0.026
1–4 van der Waals energy	2.589	2.236	2.534	2.241	1.964	2.036
van der Waals energy	−3.743	−3.160	−2.896	−1.57	−0.75	−1.76
1–4 Electrostatic energy	46.568	37.291	40.992	40.128	37.267	35.078
Electrostatic energy	−48.203	−34.014	−39.563	−38.288	−34.131	−31.492
Total Energy	10.992	13.183	13.216	15.343	18.987	19.367
Ring strain energy	13.781	10.830	12.149	12.832	14.637	15.505
Total electrostatic energy	−1.635	3.277	1.429	1.840	3.136	3.586

of view, the all-*trans* form is the only one to be explicitly stabilized by the presence of four hydrogen bonds that generate a γ-turn-like structure. It must be pointed out that these turns are generally artificially favored by in vacuo energetic computation (due to the electrostatic interaction term). Therefore the comparison of theoretical energies may not reflect the reality of peptide structure in solution, because of overestimated γ-turn conformations. Nevertheless, our computation of the cyclo(Gly)$_4$ conformations that gives the all-*trans* conformation favored (Table III) is consistent with the NMR analysis of Grathwohl and Wüthrich,[38] and thus stabilization of the various forms by hydrogen bonding fully accounts for the stability order finally obtained in the case of cyclo(Gly)$_4$. We will see thereafter that this approach (analysis of bonded and electrostatic terms) is also validated by three other experimental and theoretical conformationals studies.

Rules Predicting Conformation of Cyclic Tetrapeptides from Backbone Structure. From this first analysis, it is possible to draw few rules to predict the conformation of cyclic tetrapeptides: (1) The smallest ring tension is attained in the TCTC form. (2) The presence of γ-turns within cyclopeptide structures brings some energy stabilization, and γ-turns can be found only in the all-*trans* form. (3) The presence of N-methylations favors the TCTC form, by decreasing its energy of ring strain (a *cis* conformation is unfavorable, but N-methylation counterbalances the deficit in energy). (4) And N-methylations, by hindering the formation of γ-turns, do not favor the all-*trans* form (electrostatic term).

These rules successfully predict the reported conformations of cyclotetrapeptides such as cyclo(Sar)$_4$ and cyclo(SarGly)$_2$, which both contain N-methylations and which are found as TCTC according to Titlestad[39] (Table IV).

Influence of Side Chains: Comparison Between Computation and Conformational Analysis of Synthesized cyclo(Ala)$_4$. These first empirical rules do not address the influence of side chains on cyclotetrapeptide conformations. We show in this section that in vacuo computations can help us to understand how they impact on the stability of each conformation and thus to determine the relative proportions of conform-

Table IV Theoretical Energies of Various Forms of Four Cyclotetrapeptides and Comparison with Experimental Results

	Theoretical Total Energy in kcal · mol^{-1}						
	TTTT	TCTC	TCTT	CCTT	CCCT	CCCC	Experimental Conformation (Ref.)
cyclo(Gly)$_4$	***10.992***	13.183	13.216	15.343	18.987	19.367	TTTT (38)
cyclo(SarGly)$_2$	18.895	***18.871***	19.496	25.220	24.482	24.905	TCTC (39)
cyclo(Sar)$_4$	30.658	***25.022***	31.797	32.266	32.295	33.136	TCTC (39)
cyclo(Ala)$_4$	16.092	***15.248***	16.693	17.951	21.264	23.353	TCTC/TTTT (this work, ratio 76:24)

Table V NMR Chemicals Shifts and Coupling Constants of cyclo(Ala)$_4$ Recorded at 500.13 MHz in $CDCl_3$ at −15°C (Slow Chemical Exchange Regime)[a]

Family I (76%)					
	Chemical Shifts (ppm)			Spin–Spin Coupling Constant J (Hz)	
Residue	NH	H_α	H_β	$^3J_{H\alpha NH}$	$^3J_{H\alpha H\beta}$
Ala^1 and Ala^3	5.085	4.199	1.356	< 3.0	7.02
Ala^2 and Ala^4	6.771	4.617	1.427	7.32	7.48
Family II (24%)					
	Chemical Shifts (ppm)			Spin–Spin Coupling Constant J (Hz)	
Residue	NH	H_α	H_β	$^3J_{H\alpha NH}$	$^3J_{H\alpha H\beta}$
Ala^1 and Ala^3	5.027	4.040	1.362	< 3.0	7.17
Ala^2 and Ala^4	8.626	4.066	1.562	< 3.0	6.56

[a] Concentration of the Sample 15 m*M*

ers. In order to assess the validity of our computations, we compared theoretical predictions with experimental results on multiconformational equilibrium of the cyclic peptide cyclo(Ala)$_4$.

We first determined using TRIPOS force field, the energy in vacuo of the various forms of cyclo(Ala)$_4$ (Table IV). The simulation reveals that in an apolar solvent (chloroform) cyclo(Ala)$_4$ should be in conformational equilibrium between a major family (TCTC, 80%) and a minor one (all-*trans*, 20%).

Total synthesis of cyclo(Ala)$_4$ was needed to check the validity of this prediction. It has been achieved starting from the Boc–(Ala)$_4$–Obz precursor according to a standard cyclization protocol (pentafluorophenolate ester in diluted media,[40] see Supplementary Material). Purification through Kromasil C18-reverse phase high performance liquid chromatography (HPLC) led to a yield in cyclo(Ala)$_4$ of 10%.

Multiconformational analysis of cyclo(Ala)$_4$ was then achieved by ^{1}H-NMR spectroscopy in DCCl3 to mimic in vacuo conditions and compare with theoretical computations. We performed a study in temperature dependency, which is a convenient way to determine the composition of conformational families.[23] Indeed, a raise in temperature increases the transition rate between conformers of the same family. The ^{1}H-NMR signals of those interconverting conformers will merge at sufficiently high temperature, when the fast chemical exchange regime at the NMR time scale is reached.

In $CDCl_3$, the temperature dependency was analyzed between +35 and −15°C. Two conformers were observed throughout the whole temperature range without any change in their chemical shifts or proportions (spectra not shown). The absence of coalescence at high temperature indicated the absence of fast chemical exchange (relatively to NMR time scale) between those two conformers.

The ring conformation of the various forms in equilibrium was determined at low temperature in a slow exchange regime, by the analysis of chemical shifts and $J_{H\alpha NH}$ coupling constants derived from one-dimensional (1D) ^{1}H-NMR and two-dimensional (2D) ^{1}H-NMR correlated spectroscopy (COSY) experiments. Table V shows that two distinct sets of conformers can be observed in a 76/24 ratio. In each conformer family, two sets of chemical shifts were found, representing four alanyl residues. Both conformational families share a C2 symmetry, consistent with only all-*trans* and TCTC conformations. The major conformational family (76%) is characterized by two pairs of equivalent residues (Ala^1/Ala^3 and Ala^2/Ala^4) with chemical shifts for the Hβ split by less than 0.1 ppm, and two well-separated Hα signals ($\Delta\delta$ = 0.418 ppm). The $J_{H\alpha NH}$ coupling constants of the two pairs of equivalent residues were found to be 7 Hz and <3.0 Hz, respectively. The minor conformational family (24%) exhibits different features: Hβ chemical shifts split by 0.2 ppm, and Hα chemical shifts very close, while $J_{H\alpha NH}$ coupling constants are both lower than 3 Hz.

The major family seems to correspond to a TCTC

Table VI Dihedral Angles of Modeled All-*trans* and TCTC Conformations of cyclo(Ala)$_4$[a]

All-*trans* Form				
Residue i	1	2	3	4
ϕ_i	−71.5	65.6	−71.5	65.6
ψ_i	76.8	−70.7	76.8	−70.7
$\omega_{(i-1)-i}$	159.5	−160.3	159.5	−160.3
Calculated	3.52	1.76	3.52	1.76
TCTC Form				
Residue i	1	2	3	4
ϕ_i	−55.3	−146.9	−55.3	−146.9
ψ_i	−35.4	91.3	−35.4	91.3
$\omega_{(i-1)-i}$	2.7	−176.5	2.7	−176.5
Calculated	2.08	6.82	2.08	6.82

[a]The theoretical coupling constants $^3J_{H\alpha NH}$ (Hz) were calculated according to the Karplus relation corrected as in Ludwigsen *et al.*[49]

ring conformation, while the minor one represents the all-*trans* form. Indeed, in the TCTC conformation, the environment of the two $CH_3\beta$ groups of each pair of equivalent alanines differ only by the orientation of the adjacent carbonyl group (leading to a split lower than 0.1 ppm), whereas in the case of the all-*trans* form, the carbonyl and the amide nitrogen both participate in the magnetic non-equivalence of the Hβ protons ($\Delta > 0.2$ ppm). This is confirmed by the analysis of the Hα chemical shifts. For the TCTC conformation, two protons are significantly low-field shifted due to the vicinity of the carbonyl group, leading to the existence of two distinct classes of chemical shifts. In the all-*trans* forms, the environment of the Hα protons is similar, giving rise to only one set of chemical shifts. An analysis of the $J_{H\alpha NH}$ coupling constants obtained theoretically and experimentally (Tables V and VI) confirms that the major form is associated to a TCTC ring conformation while the minor form corresponds to an all-*trans* conformation.

In water, the same study was achieved between 5 and 85°C. At 5°C, four conformers can be distinguished (A: 50%; B: 32.8%; C: 14.4%; D: 2.8%). While increasing temperature, the chemical shifts of the forms B, C and D merged, indicating an evolution from slow to fast chemical exchange. It appears therefore that those forms (B, C and D) belong to the same conformational family. The form A, whose chemical shifts and proportions remain unchanged with temperature, is not in fast chemical exchange with the other forms and thus belongs to another conformational family. The absence of conformational transition between the two sets of conformations, A and B+C+D, corresponds to an activation energy higher than 30 kcal · mol^{-1}.

In conclusion, the predicted conformations match, qualitatively and quantitatively, those observed experimentally. This validates the computational approach. Moreover, the TRIPOS force field and its parameterization allowed us to avoid the common artifact of generating γ-turns, often encountered in other molecular mechanics experiments.

Tentoxin Model. The six possible backbone forms have been built and optimized for tentoxin molecule (Table VII). The results indicate that TCTC family presents the lowest total energy, and that, in contrast, the all-*trans* is one of the less stabilized conformations. It has been mentioned above that electrostatic contribution in cyclo(Gly)$_4$ was a strong stabilizing factor in favor of the all-*trans* form due to the presence of four γ-turns. Conversely, in tentoxin, the electrostatic term does not promote the all-*trans* form, as a direct consequence of the presence of two N-methylations that precludes the formation of intramolecular hydrogen bonds. In addition, the ring strain of TCTC conformation is found to be the lowest among the six forms. The TCTC ring strain is found significantly lowered in the case of tentoxin when compared to cyclo(Gly)$_4$, because in cyclo(Gly)$_4$ the conversion of two peptide bonds from *trans* to *cis* con-

Table VII Energy Terms (in kcal/mol) of the Six Different Minimized Backbone Conformations of Tentoxin

	TTTT	TCTC	TCTT	CCTT	CCCT	CCCC
Bond stretching energy	2.259	2.246	1.992	2.776	2.955	2.602
Angle bending energy	11.924	6.898	7.164	11.576	17.730	10.843
Torsional energy	33.121	23.510	31.721	24.419	33.176	27.459
Out-of-plane bending energy	1.418	0.416	0.860	0.636	2.101	0.448
1–4 van der Waals energy	5.969	4.462	4.332	4.601	6.025	4.389
van der Waals energy	−7.092	−7.154	−7.678	−5.616	−8.058	−6.365
1–4 electrostatic energy	37.678	38.934	38.503	37.658	33.635	34.560
Electrostatic energy	−31.577	−28.688	−31.990	−30.697	−26.518	−26.328
Total energy	53.699	40.625	44.902	45.352	61.046	47.606
Ring strain energy	48.722	33.070	41.737	39.407	55.962	41.352
Total electrostatic energy	6.101	10.246	6.513	6.961	7.117	8.232

formations to generate the TCTC form has an energetical cost that is not counterbalanced by the presence of N-methylations. In N-methylated peptide bonds, the energies of *cis* and *trans* conformations are indeed comparable.[41] Last, when comparing the values of van der Waals energy terms, it can be noticed that side chains are less sterically bulky in TCTC and TCTT conformations.

In conclusion, the presence of side chains and of N-methylation both contribute to favor the TCTC family in the cyclotetrapeptide. This result is in full agreement with the data derived from tentoxin NMR analysis.[26]

Subconformations in TCTC Backbone Conformation Family

The alternate TCTC defines the predominant backbone conformation of tentoxin. But within this conformation, it is still possible to generate a significant number of subconformers. Only four of them have been observed and determined in aqueous solution.[26] If we except the variety of configurations that can arise from side chains, the orientation of carbonyl groups of ring peptide bonds is the main foundation of the conformational variety in cyclopeptides. In the present example, each carbonyl group can be U or D oriented. For only one backbone conformation such as TCTC, this represents sixteen subconformers (Figure 5), on which we can perform an empirical structural analysis, as well as an energetic analysis.

Empirical Approach. In the ring of a cyclic molecule, the substituents of sp^3 carbons are either in the axial or equatorial position. The latter is favored because it allows stabilization of the ring.

According to the Dunitz–Waser representation of the cyclic tetrapeptide, which adopts a TCTC conformation,[42] we can assimilate side chains of the cyclic tetrapeptide to cyclohexane substituents. For the cyclohexane, the axial position of substituents induces some steric hindrance. This favors conformation with substituents in equatorial position. Identically, in cyclic tetrapeptide, the axial orientation of side chain creates transannular interactions[43] that are not observed in equatorial position.

In the tentoxin structure, only the side chains of amino acids L-MeAla[1] and L-Leu[2] are concerned, since the third residue is [Δ(Z)]Phe (sp^2 carbon) and the fourth is Gly (no side chain). The orientation of *cis* peptide bond planes fully controls the position of the vicinal side chains. The *cis* peptide bonds that are upper-side directed impose an equatorial orientation of side chains, whereas lower-side directed impose axial orientation of substituents. In tentoxin, where substituted amino acids are residues 1 and 2, the carbonyl groups of closest *cis* peptide bonds that control the positions of their side chains belong to amino acid 4 (Gly) and 2 (L-Leu), respectively. In Figure 5, we can notice the axial or equatorial features of side chains of residues 1 and 2 for each of the sixteen conformers of the TCTC family. Among them, eight (colored in blue) exhibit one of their two side chains in axial position, four (in red) exhibit both side chains in axial position, and four (in black) exhibit both side chains in equatorial position. These four latter ones should be, as a consequence, energetically the most favored conformers. This empirical

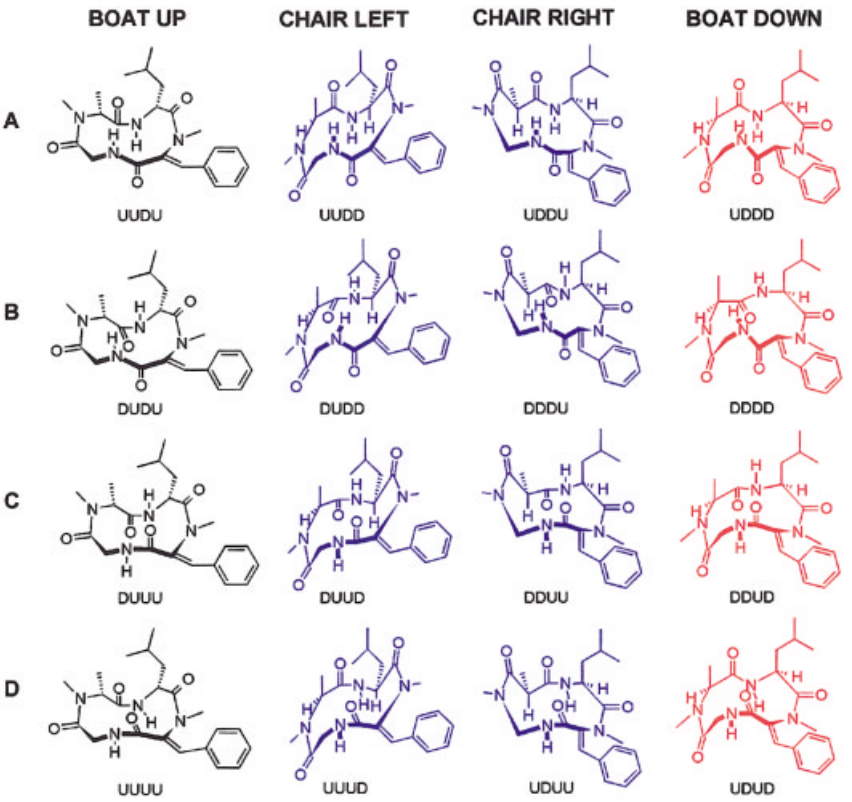

FIGURE 5 Schematic representation of sixteen conformations for cyclic tetrapeptide TCTC backbone conformation. Four families : BOAT UP (xUxU), CHAIR LEFT (xUxD), CHAIR RIGHT (xDxU), and BOAT DOWN (xDxD), arranged in columns; and four series A (UxDx), B (DxDx), C (DxUx), and D (UxUx), arranged in lines.

analysis allows us to predict that only one group of subconformers exists in solution: these are the BOAT UP conformers. They correspond exactly to those observed experimentally by NMR.[26]

Molecular Mechanics Approach. This stabilization of BOAT UP conformers can be demonstrated also by energy minimization performed in vacuo on each of the sixteen subconformers of the TCTC family. Each structure has been optimized by restrained molecular dynamics simulations (using constraints tabulated in Table S1 of the Supplementary Material) at 100 K during 1000 fs as described in experimental procedures. Table VIII reports the corresponding energies computed by molecular mechanics. The data revealed that conformers named A–C by E. Pinet et al. and belonging to the BOAT UP forms, were indeed those of lowest energy, in complete agreement with the above empirical approach. The corresponding energies, however, do not reflect the stability order found in solution, where A was experimentally the major form, instead of C. Moreover, the next more stable conformer was found to be the C-CHAIR RIGHT-DDUU (for conformational nomenclature of cyclic TCTC tetrapeptide, see Material and Methods) according to computed energies, and not the D-BOAT

Table VIII Energy (in kcal/mol) of the Sixteen TCTC Conformations of Tentoxin Minimized *In Vacuo*

	BOAT UP	CHAIR LEFT	CHAIR RIGHT	BOAT DOWN
A	41.518	42.533	44.343	42.559
B	39.711	48.405	45.12	51.363
C	39.338	45.789	42.018	43.762
D	49.052	48.552	49.781	45.346

UP-UUUU that was expected from the NMR analysis. The presence of the latter form was actually proposed by Pinet et al. as a logical consequence of the conformational equilibria found to occur in solution between the three other BOAT UP conformers, but there was no direct experimental evidence. The discrepancy between the fourth stable conformer predicted by molecular mechanics analysis and the fourth hypothetical conformer D-BOAT UP suggested by NMR analysis can nevertheless be explained by the fact that the computation did not take into account the role of the solvent, while it is clear from the data of Table II that the stability order of conformers in solution depends strongly on the nature of the solvent (B was found to be the major form in chloroform, whereas A was predominant in water). Thus, the energetic analysis, to be more exhaustive, needs to include the solvent contribution.

Within each horizontal series A–D of Figure 5, the stability order derived from energies was also not always consistent with the empirical determination. BOAT UP forms were found globally more stable than CHAIR LEFT, CHAIR RIGHT, and BOAT DOWN. But in the A conformer series (UxDx conformers), it can be seen that UDDD, a form exhibiting two side chains in the axial position, is energetically more stable than UDDU, which presents only the leucine side chain in the axial position. This is due to a down side movement of the *cis* peptide bond between glycine and alanine, which generates a ring strain that reduces the nonbonded (hydrophobic) interaction between leucine and dehydrophenylalanine side chains. In series B (DxDx conformers), the stability order derived from energies was very consistent with the empirical one. In series C (DxUx conformers), for the same reasons of ring tension as in the A series, the DDUD form was energetically more stable than the DUUD form. Lastly, in series D (UxUx conformers), the stability order was found to be BOAT DOWN > CHAIR LEFT > BOAT UP > CHAIR RIGHT, indicating that in this series the ring strain controls significantly the energetic stability. It can be seen that, among the TCTC conformers, the stability is controlled by the ring strain and the transannular interactions linked to the side-chain orientation.

In summary, the empirical approach based on the number of axial and equatorial orientations of lateral groups gave results consistent with the conformations found in solution. The mechanistic approach in vacuo was as satisfactory, since the three most energetically stabilized conformers were also the conformers A-BOAT UP-UUDU, B-BOAT UP-DUDU, and C-BOAT UP-DUUU. It appears now necessary, in order to refine the prediction on stability order and to resolve the proportion of each conformer, to take into account the solvent contribution. This was realized following two strategies, either by including the dielectric constant of the solvent in given experimental conditions, or by constructing solvated systems of the solute conformers.

Taking into Account the Solvation Effects

We have chosen two usual methods (SCRF or solvent box method) to simulate the solvent effects and to evaluate which parameters would influence the stability of each conformational state—especially, the dielectric constant for the solvents that do not interact with tentoxin by hydrogen bonds, and the direct interaction solvent/solute for the solvents that chelate tentoxin through hydrogen bonds.

Solvation Using a Dielectric Field. In first approximation, the solvent can be modeled by including a simple distance-dependent dielectric constant function in calculations, to simulate the effect of the solvent by its electrostatic contribution. This approach is, however more, legitimate when the solvent does not strongly interact with the solute molecule to be modeled. Concerning tentoxin conformer population, the solvents for which we had the most precise NMR data at our disposal, were D_2O and $DCCl_3$. In our calculations, we took into account the temperature dependence of dielectric constant, expressed by the following equation[44]:

$$\varepsilon = a + b.\mathrm{T} + c.\mathrm{T}^2$$

(the values of parameters a, b, and c are detailed in Table S2 of the Supplementary Material for water and chloroform).

As the corresponding data for deuterated chloroform were not found in literature, we used the parameters tabulated for $HCCl_3$, a reasonable approximation since there is no appreciable divergence between H_2O and D_2O reported parameters. The temperature domain valid for D_2O parameters ranges from 277.2 to 373.2 K, whereas the chemical exchange NMR study of Pinet et al. has been realized between 268 and 358 K, in aqueous salted solution (0.2*M* NaCl). We neglected the influence of this salt concentration on dielectric constants, and extended their validity domain down to 268 K to obtain the values of dielectric constants of water and chloroform at different temperatures.

Table IX Energy (in kcal/mol) of the Sixteen TCTC Tentoxin Conformations Minimized According to the Solvent Dielectric Constant

Solvent:	D_2O	D_2O	$DCCl_3$
Temperature:	85°C	−5°C	−45°C
ε:	59.23	89.49	14.79
A-BOAT UP	31.017	30.944	31.373
B-BOAT UP	29.405	29.343	29.950
C-BOAT UP	31.065	31.014	31.515
D-BOAT UP	37.263	37.191	37.913
A-CHAIR LEFT	32.691	32.631	33.241
B-CHAIR LEFT	37.380	37.310	37.984
C-CHAIR LEFT	39.710	39.673	40.053
D-CHAIR LEFT	38.872	38.810	39.394
A-CHAIR RIGHT	36.647	36.598	37.059
B-CHAIR RIGHT	36.883	36.836	37.329
C-CHAIR RIGHT	33.412	33.361	33.906
D-CHAIR RIGHT	37.840	37.760	38.494
A-BOAT DOWN	35.277	35.235	35.682
B-BOAT DOWN	41.560	43.178	42.098
C-BOAT DOWN	35.444	35.396	35.908
D-BOAT DOWN	35.416	35.370	35.949

The solvation effect as viewed by the dielectric constant was investigated on the sixteen conformers of TCTC family, as defined in the previous section. Energy minimizations were carried out on each optimized structure using the adequate dielectric constant parameters (solvent, temperature). The results are displayed Table IX. It is noteworthy that the four most stabilized conformers were the same, whatever the solvent and temperature conditions: these were, again, A–C forms from the BOAT UP family, and the fourth stabilized form was found to be A-CHAIR LEFT-UUDD, and not the D form of BOAT UP family. From relation (4), we determined the proportions of these five specific conformers (Table X). To limit inaccuracy on energy value obtained for each conformational state, we minimized each conformation up to a gradient termination of 0.05 kcal $\cdot$ mol^{-1} $\cdot$ Å $^{-1}$, which corresponds to an inaccuracy lower than 1% of the population.

Not surprisingly, the simulation of solvent effect by the distance-dependent dielectric constant function only slightly improved the precision of the results. This approach failed in particular for water conditions, in which B-BOAT UP was found energy stabilized, when A-BOAT UP is the predominant form in solution NMR. As already mentioned, the use of the dielectric constant is adequate only in the absence of strong interaction between solvent and solute molecules. Water is a protic solvent likely to establish hydrogen-bond-like interactions with cyclopeptides. For the conformational study of tentoxin in water, it is therefore necessary to account for possible strong interactions with solvent molecules, by implementing a solvated system-like approach.

In the case of chloroform, we obtained significantly better results in terms of conformer populations (Table X), in agreement with the fact that interactions of chloroform with cyclopeptides are weaker. In $CDCl_3$, the energetical simulations gave the B-BOAT UP-DUDU as the major conformer, in agreement with data derived from NMR spectra recorded in slow chemical exchange conditions at −45°C. In a decreasing stability order, A-BOAT UP-UUDU and C-BOAT UP-DUUU are then found. This is still in complete agreement with the populations measured from NMR studies at −45°C (Table II). It is noteworthy that 92% of B-BOAT UP-DUDU, 4% of A-BOAT UP-UUDU, and 2% of C-BOAT UP-DUUU were predicted using the dielectric constant approach, when experimentally these were found respectively present at 86, 13, and 0%. The predominance of B-BOAT UP-DUDU in chloroform is very well predicted, as well as the hierarchy between the other observed forms, as shown by the energies. The weak deviations could arise from possible weak association solute/solvent between tentoxin and chloroform, but they more likely result from force field limitations.

Though this method gave satisfactory results in the case of chloroform, it seems now interesting to consider more markedly the interaction solvent/solute, by

Table X Deduced Proportions of the Five Most Stable Conformations After Simulation Under a Solvated System According to SCRF Method[a]

Solvent	Temp.	ε	A-BOAT UP	B-BOAT UP	C-BOAT UP	D-BOAT UP	A-CHAIR LEFT
D_2O	85°C	59.23	8.6	82.6	8.0	0.0	0.8
D_2O	−5°C	89.49	4.5	91.3	4.0	—	0.2
$DCCl_3$	−45°C	14.79	4.0	93.0	3.0	—	0.0

[a] Simulation in deuterated water and chloroform.

Table XI Energy (in kcal/mol) and Proportions of Four TCTC Conformations Observed in Deuterated Water After Simulation Under a Solvated System According to SILVERWARE© Method

	Temperature: 85°C			Temperature: −5°C		
	Total Energy (in kcal · mol^{-1})	Computed Proportions	Experimental Proportions	Total Energy (in kcal · mol^{-1})	Computed Proportions	Experimental Proportions
A-BOAT UP	−207.982	52.6	44	−205.921	57.1	51
B-BOAT UP	−207.849	43.7	39	−205.755	41.8	37
C-BOAT UP	−206.101	3.7	16	−203.812	1.1	8
D-BOAT UP	−200.633	—	—	−198.572	—	4

taking into account both the electrostatic interactions (through the dielectric constant) and the nonbonded van der Waals interactions between tentoxin and solvent molecules (water or chloroform).

Simulation by Solvated System. Both experimentally and analytically, the forms of BOAT UP family proved to be the most stabilized (except D, but this form was not explicitly observed in NMR). In this last molecular mechanics approach, we focused on the four conformers of this predominant family to test the robustness of the prediction on conformer populations, both in water and chloroform. Solvated systems were realized by building a solvent molecular box using the solvation algorithm DROPLET. The built systems were composed of tentoxin conformer surrounded by two layers of H_2O molecules, to which were assigned the dielectric constant values found for D_2O. After minimization, the energy value of the conformer in each solvated system was extracted and utilized to determine the proportions according to relation (4). The results are displayed in Table XI. It can be seen that a very good agreement was this time attained in water between calculated values and experimental values. A and B conformer populations were found slightly higher than the experimental populations (deviation less than 10%) to the detriment of C and D conformers, D being insignificantly populated according to the computation. The progression of conformer proportions as a function of temperature is also well predicted. Indeed, the experimental and calculated values evolve analogously between the two limit temperatures: when temperature increases, the proportion of A decreases, that of B increases and the proportion of C is doubled. The development of conformer populations as a function of temperature was thus well reproduced. This very good agreement obtained in water, as opposed to the previous simulation performed using the sole dielectric constant effect, strongly suggests that water molecules interact with the cyclotetrapeptide, by differentiated stabilization of the various conformers in solution. These solvent/solute interactions contribute to significant changes in conformer populations. The residual differences observed between computed and experimental proportions in water can arise from several parameters such as the presence of sodium chloride salt (ignored in the simulation) or the approximations on dielectric constant parameters. Yet, the population values determined according to the solvated system approach were found remarkably consistent with experimental data.

To confirm the superiority of this last approach, we also carried out the simulations in chloroform. Results are reported in Table XII. The consistency with experimental values was even improved: computed and experimental values differed by less than 5%, on the four BOAT UP conformers, which is remarkable for a molecular mechanics approach.

The TRIPOS force field, associated with DROPLET method of solvation based on SILVERWARE© algorithm, appeared quite appropriate to account en-

Table XII Energy (in kcal/mol) and Proportions of Four TCTC Conformations Observed in Deuterated Chloroform at −45°C After Simulation Under a Solvated System According to SILVERWARE© Method

	A-BOAT UP	B-BOAT UP	C-BOAT UP	D-BOAT UP
Total energy (in kcal · mol^{-1})	−425.540	−426.572	−423.437	−420.469
Computed proportions	9.3	90.6	0.1	—
Experimental proportions	13	86	—	—

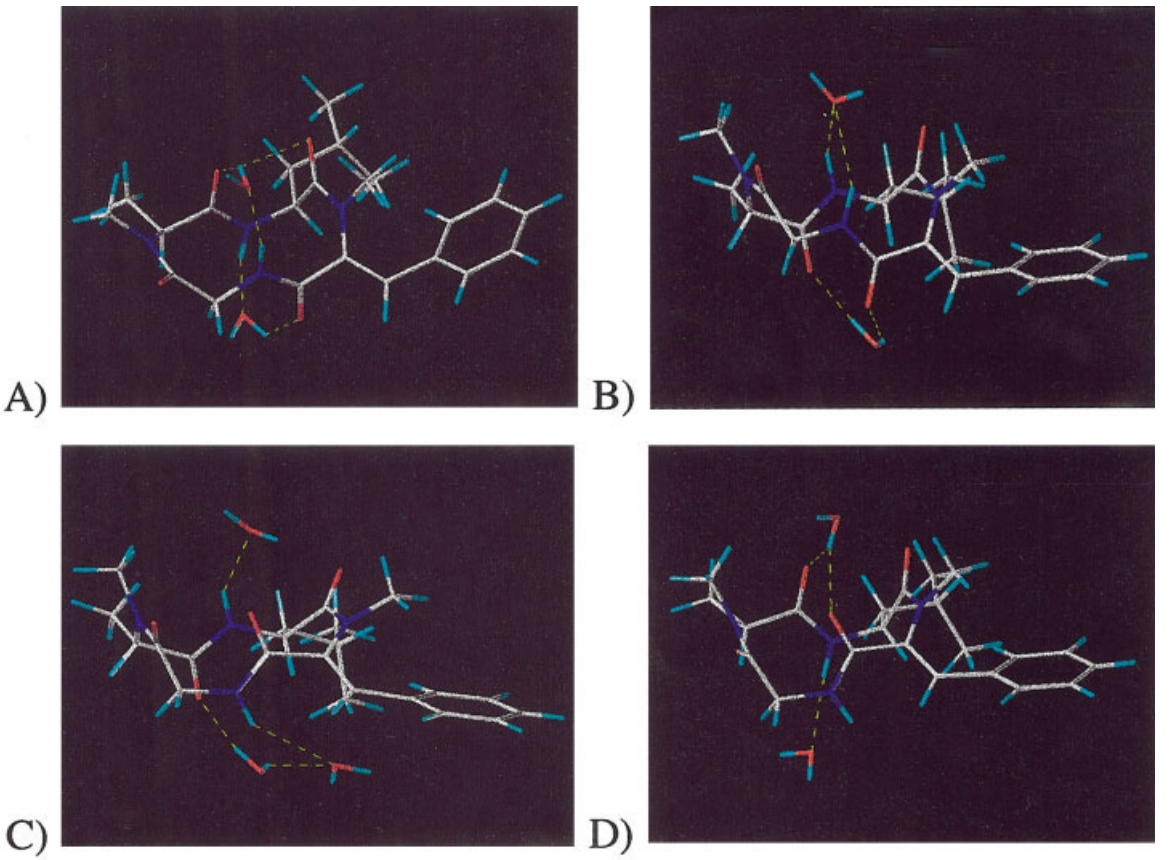

FIGURE 6 Hydrogen bonds between the solute (tentoxin) and the solvent (water). Chelation pattern in water of tentoxin: (A) A-BOAT UP form, (B) B-BOAT UP form, (C) C-BOAT UP form, and (D) D-BOAT UP form.

ergetically for conformer populations experimentally determined in solution.

Solvated System Analysis. To complete this study with an exhaustive analysis of solvated systems, our aim was to understand the phenomenon involved in the stabilization of A and C BOAT UP conformers in water.

In chloroform, results based only on dielectrical constant approach (the section, Solvation Using a Dielecric Field, above) are similar to the ones obtained by the solvated systems method. This confirms the poor number of solute/solvent interactions when tentoxin is dissolved in chloroform. The improvement of the prediction observed with the latter method may result from a more accurate force field linked to a more adequate repartition of the charges.

In water, the main improvement of the solvated system method resides in the integration of the hydrogen-bond network. In order to analyze the direct interactions between tentoxin and water, we focused, for each simulation, on tentoxin and water molecules interacting through hydrogen bonding. The main difference in the solvation of tentoxin conformers resides in the type of hydrogen bonding between secondary peptide bonds and solvent (Figure 6).

For the conformers A- and C-BOAT UP, each side of the tentoxin mean plane presents an amide bond (NH, Lewis acid) and a carbonyl group (CO, Lewis base). The BOAT UP ring conformation is too constrained to allow an intramolecular hydrogen bonding between those groups that can therefore freely interact with water molecules. Consequently, on each side of tentoxin, one or two water molecules can interact with tentoxin leading to a strong chelation (Figure 6). The strong stabilization obtained by hydrogen-bonded water molecules is explained by the electronic conjugation than can occur [Scheme 2(panel A)]. For conformer C, the possibility of conjugation is diminished, due to the fact that the simulation found two water molecules bonded on the lower side (Figure 6). This may explain that the proportion of C was less well predicted (Table XI).

A contrario, for B and D conformations, the CO

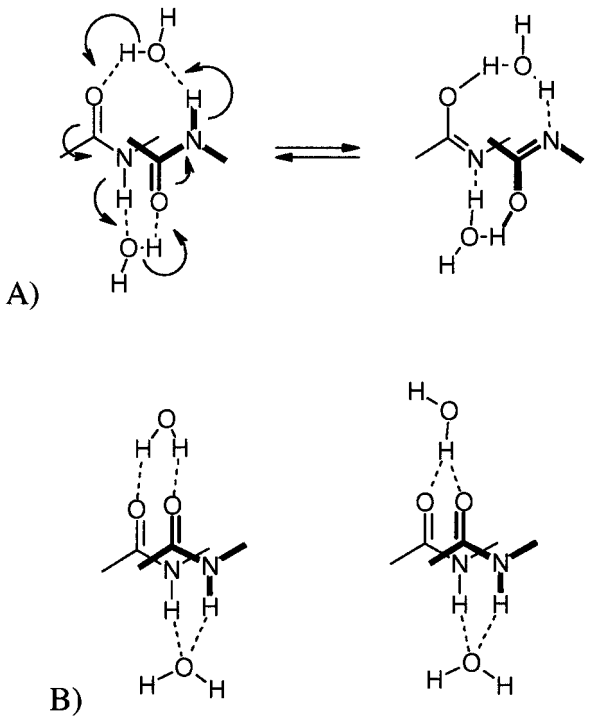

SCHEME 2 Water/tentoxin interactions in A–D forms of TCTC conformation. (A) Stabilization of water-chelated A and C forms through electronic conjugation. (B) Water-chelated B and D forms are not stabilized by conjugation.

groups of the secondary peptide bonds are located on the same side of tentoxin mean plane, and the corresponding NH groups on the other side. These two amide protons are connected with an oxygen of a unique water molecule. On the other side, the oxygen of the two carbonyl groups is also engaged in an hydrogen bond with two protons of a unique water molecule. [Scheme 2 (panel B)]. The A-type interaction (Scheme 2) involves a greater number of hydrogen-bonded atoms than the B-type does. This strengthens hydrogen-bonding network and increases the stability of the conformation. But, in the B-type, no electronic conjugation can occur.

Therefore B- and D-BOAT UP conformations are less stabilized by solute/solvent interactions than A and C conformations are. Besides, this analysis can also explain the high energy obtained for the D conformer during the minimization of the solvated system. This solvated conformer presents indeed B-type interaction (which is less stabilizing) and only one amide proton is associated with a water molecule.

Model for Solvation of Cyclotetrapeptides. The same analysis of tentoxin solvated systems allowed us to define a solvation model for each form of tentoxin. Solvents can be classified along three types: apolar aprotic, polar protic, and polar aprotic. The apolar aprotic solvents (for example, chloroform) do not interact directly with tentoxin. In that case, the B-BOAT UP conformation should be the most stable. The polar and protic solvents (like water), display X—H dipoles (where X is an heteroatom like oxygen, sulfur, or nitrogen) susceptible to strongly interact with tentoxin. For these solvents, the A-BOAT UP conformation should be the most stable. Finally, the polar and aprotic solvents (dimethyl formamide, DMSO, etc.) carry heteroatoms that are likely to interact with amide protons of secondary peptide bonds. These solvents should consequently favor the B- and D-BOAT UP conformations of tentoxin, where amide protons are located on the same side of the average plane.

In order to confirm this prediction, we studied the effect of DMSO on the conformations of tentoxin. We observed the effect of DMSO addition on the conformational equilibrium of tentoxin dissolved in chloroform. The study was achieved through 1D ^{1}H-NMR experiments carried out at 250 K. This temperature allows us to slow down the chemical exchange on the NMR time scale, and all conformers can be observed separately.

Figure 7A shows the repartition between tentoxin conformers A- and B-BOAT UP (respectively 13 and 8 %) in the spectral region corresponding to tentoxin aliphatic protons. Addition of small amount of DMSO (3%) drastically modified the tentoxin conformational equilibrium (Figure 7B). It induced indeed the complete disappearance of conformer A-BOAT UP to the benefit of conformer B-BOAT UP. This phenomenon could have resulted from an increase in the rate of chemical exchange: since B-BOAT UP is overwhelmingly the major conformer, coalescence of NMR signals would have led to a final spectrum similar to the one of B-BOAT UP conformer. We would have observed therefore an important shift in the δ leucine protons. But the chemical shifts of all protons (including those of leucine) are rigorously the same before and after addition of DMSO. Therefore, the effect of DMSO does not correspond to an acceleration of the chemical exchange, but rather to a stabilization of the conformer B-BOAT UP that leads to the disappearance of conformer A. This confirms our predictions of the effects of polar and aprotic solvents on tentoxin conformational equilibrium and therefore validates our theoretical approach of cyclotetrapeptide solvation phenomenon.

CONCLUSION

The theoretical approach on cyclotetrapeptide conformations presented in this work, validated on the well-

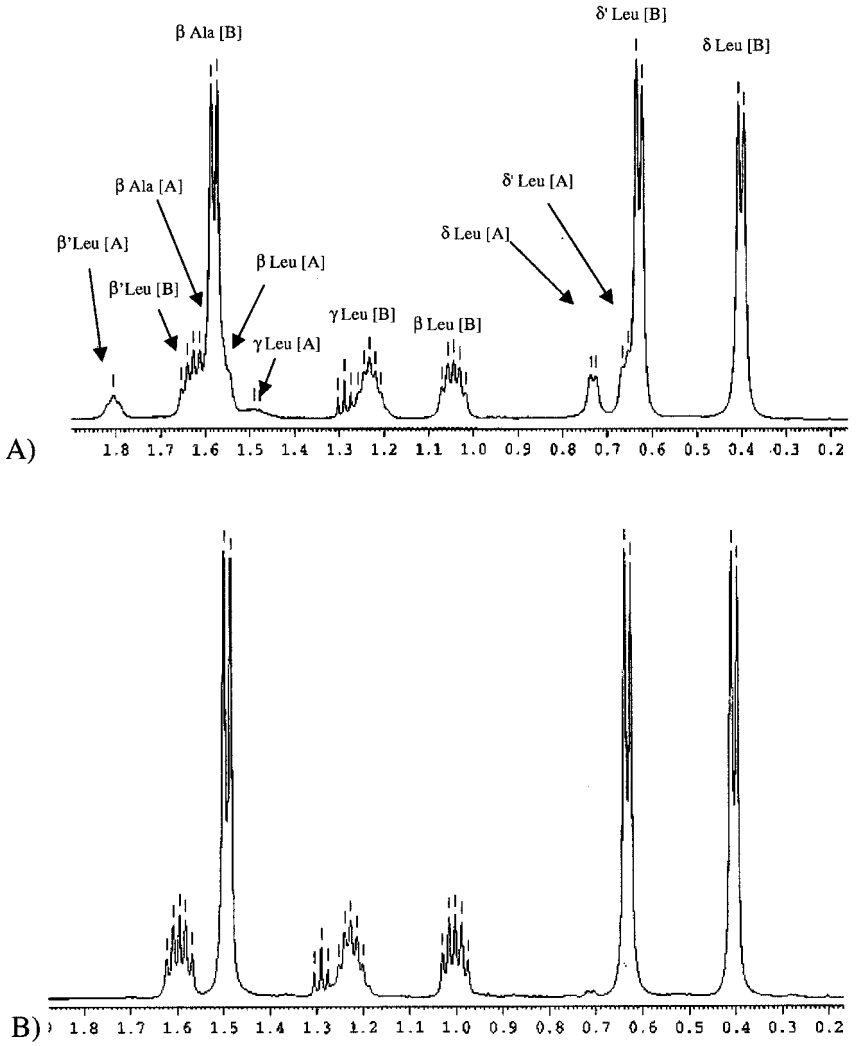

FIGURE 7 Stabilization of tentoxin B-BOAT UP form in DMSO. Panel A: aliphatic region of the ^{1}H-NMR spectrum of tentoxin 1 m*M* recorded at 500 MHz in CDCl3 at −20°C. Protons corresponding to conformers A and B (ratio 13/87) are indicated. Panel B: spectrum recorded in the same conditions after addition of 3% DMSO.

documented example of the phytotoxic cyclotetrapeptide tentoxin, yielded results in complete agreement with the experimental data. The minor deviations observed seem to result from the approximation used in computing dielectric constants. By comparison to the empirical rules proposed by Kato, the method we described here, based on the potential energy values of each conformer derived from molecular mechanics approach, allow us to determine, with a good accuracy, the proportions of the various conformers present in solution, in various temperature and solvent conditions. The whole work has been carried out without introducing the experimental NMR data, which were requested only to validate the quality of the results derived from the predictive method. In the case of tentoxin, it is clear that a strong interaction occurs with the solvent. Thus, a hydrophobic environment stabilizes the B-BOAT UP form, and a hydrophilic medium stabilizes A-BOAT UP and C-BOAT UP forms. This result is particularly valuable for the prediction of bound conformation of the toxin in its enzymatic target active site. The predictive approach gives here essential keys to the investigation of the interaction of tentoxin with various enzyme complexes, such as the chloroplast F_0F_1 ATP-synthase, its natural target, and the mammalian cytochrome P450-3A,[45] which metabolizes it. It is noteworthy that our computational method could predict that the D-BOAT UP form, suggested by Pinet et al. as a possible fourth conformer of tentoxin occurring in solution, was neg-

ligible. This result led us to reconsider its existence in water, and a more recent NMR investigation carried out in our laboratory confirmed that the weak signals originally assigned to the D form were in fact due to some residual E-isomerization of the dehydro residue. The predicting approach by molecular mechanics simulations can be easily extended to other cyclotetrapeptides, knowing that the interactions solute/solvent mainly involve CO groups and NH groups of nonmethylated peptide bonds, as demonstrated in tentoxin. These stabilizing interactions are directly related to the predominant ring conformation (TCTC in the case of tentoxin).

This work has been supported in part by the CNRS (grant Physique-Chimie du Vivant, PCV97-185), by the Ministère de l'Éducation Nationale, de la Recherche et de la Technologie, contract ACC-SV5 No. 9505221, and by the program "Environnement-Santé" from the Ministère de l'Aménagement du Territoire et de l'Environnement (no. AC009E).

Thanks are also due to O. Richard for his help in generating Figure 3A, to A. Sanson and J.-M. Neumann for discussions and assistance in modeling.

Supplementary Material: Description of cyclo$(Ala)_4$ synthesis pathway (Scheme S1). Constraints in degrees used for dihedral angles of the tetrapeptide ring, required for conformer building and optimization (Table S1). Parameters for dielectric constant computations (Table S2).

REFERENCES

1. Templeton, G. E. Microb Toxins 1972, 8, 160–163.
2. Fulton, J. P. Phytopathology 1960, 50, 574–578.
3. Ueno, T.; Hayashi, Y.; Nakashima, T.; Fukami, H.; Nishimura, S.; Kohmoto, K.; Sekiguchi, A. Phytopathology 1975, 65, 82–83.
4. Okuno, T.; Ishita, Y.; Samai, K.; Matsumoto, T. Chem Lett 1974, 635–638.
5. Takayama, S.; Isogai, A.; Nakata, M.; Suzuki, H.; Suzuki, A. Agric Biol Chem 1984, 48, 839–842.
6. Hirota, A.; Suzuki, A.; Suzuki, H.; Tamura, S. Agric Biol Chem 1973, 37, 643–647.
7. Hirota, A.; Suzuki, A.; Tamura, S. Agric Biol Chem 1973, 37, 1185–1189.
8. Pringle, R. B. Plant Physiol 1970, 46, 45–49
9. Kawai, M.; Rich, D.-H.; Walton, J. D. Biochem Biophys Res Commun 1983, 111, 398–403.
10. Kawai, M.; Rich, H. Tetrahedron Lett 1983, 48, 5309–5312.
11. Brosch, G.; Ransom, R.; Lechner, T.; Walton, J. D.; Loidl, P. Plant Cell 1995, 7, 1941–1950.
12. Hirota, H.; Suzuki, A.; Aizawa, K.; Tamara, S. Agric Biol Chem 1973, 37, 955–956.
13. Closse, A.; Huguenin, R. Helv Chim Acta 1974, 57, 533–545.
14. Liech, J. M.; Sweeley, C. C.; Staffeld, G. D.; Anderson, M. S.; Webber, D. J.; Scheffer, R. P. Tetrahedron 1982, 38, 45–48.
15. Itazaki, H.; Nagashima, K.; Sugita, K.; Yoshida, H.; Kawamura, Y.; Yasuda, Y.; Matsumoto, K.; Ishii, K.; Uotani, N.; Nakai, H.; et. al. J Antibiot 1990, 43, 1524–1532.
16. Darkin-Rattray, S. J.; Gurnett, A. M.; Myers, R. W.; Dulski, P. M.; Crumley, T. M.; Allocco, J. J.; Cannova, C.; Meinke, P. T.; Colletti, S. L.; Bednarek, M. A.; Singh, S. B.; Goetz, M. A.; Dombrowski, A. W.; Polishook, J. D.; Schmatz, D. M. Proc Natl Acad Sci 1996, 93, 13143–13147.
17. Umehara, K.; Nakahara, K.; Kiyoto, S.; Iwami, M.; Okamoto, M.; Tanaka, H.; Kohsaka, M.; Aoki, H.; Imanaka, H. J Antibiot 1983, 36, 478–483.
18. Omar, S.; Tenenbaum, L.; Manes, L. V.; Crews, P. Tetrahedron Lett. 1988, 29, 5489–5499.
19. Aracil, J. M.; Badre, A.; Fadli, M.; Jeanty, G.; Banaigs, B.; Francisco, C.; Lafargue, F.; Heitz, A.; Aumelas, A. Tetrahedron Lett 1991, 32, 2609–2612.
20. Kawagishi, H.; Somoto, A.; Kuranari, J.; Kimura, A.; Chiba, S. Tetrahedron Lett 1993, 34, 3439–3440.
21. Kessler, H. Angew Chem Int Ed Engl 1982, 21, 512–523.
22. Kato, T.; Lee, S.; Shimohigashi, Y.; Tone, A.; Kodera, Y.; Izumiya, N. Int J Peptide Protein Res 1987, 29, 53–61.
23. Pinet, E. Thesis, Biophysique Moléculaire, Paris VI, 1996.
24. Rich, D. H.; Bathnagar, P. K.; Jasensky, R. D.; Steele, J. A.; Uchytil, T. F.; Durbin, R. D. Bioorg Chem 1978, 7, 207–214.
25. Rich, D. H.; Bathnagar, P. K. J Am Chem Soc 1978, 100, 2212–2218.
26. Pinet, E.; Neumann, J. M.; Dahse, I.; Girault, G.; André, F. Biopolymers 1995, 36, 135–152.
27. Clark, M.; Cramer, R.; Van Opdenbosch, N. J Comp Chem 1989, 10, 982–1012.
28. Berthod, H.; Pullman, A. J Chem Phys 1965, 62, 942–946.
29. Powell, M. J. D. Math Program 1977, 12, 241–254.
30. Karelson, M. M.; Katritzky, A. R.; Zerner, M. C. Int J Quantum Chem 1986, 20, 521–527.
31. Blanco, M. J Comp Chem 1991, 12, 237–247.
32. Gilson, M. K.; Sharp, K. A.; Honig, B. H. J Comp Chem 1987, 9, 327–335.
33. Alkorta, I.; Villar, H. O.; Perez, J. J. J Comp Chem 1993, 14, 620–626.
34. Gilson, M. K.; Sharp, K. A.; Honig, B. H. J Comp Chem 1987, 9, 327–335.
35. Jirousek, M. R.; Mazza, S. M.; Salomon, R. G. J Org Chem 1988, 53, 3688–3695.
36. Eliel, E. L.; Allinger, N. L.; Angyal, S. J.; Morrison, G. A. Conformational Analysis; American Chemical Society: Washington, DC, 1981; p 24.
37. Ramakrishnan, C.; Sarathy, K. P. Biochim Biophys Acta 1968, 168, 402–410.

38. Grathwohl, C.; Tun-Kyi, A.; Bundi, A.; Schwyzer, R.; Wüthrich, K. Helv Chim Acta 1975, 58, 415–423.
39. Titlestad, K. Acta Chem Scand B 1975, 29, 153–167.
40. Schmidt, U.; Lieberknecht, A.; Griezzer, H.; Talbiersky, J. J Org Chem 1982, 47, 3261–3264.
41. Dietrich, B.; Viout, P.; Lehn, J. M. Aspects de la chimie des composés macrocycliques; Savoirs Actuels, InterEditions, Edition du CNRS, Paris: 1991; p 220.
42. Kessler, H.; Gratias, R.; Hessler, G.; Gurrath, M.; Müller, G. Pure & Appl. Chem., 1996, 68, 1201–1205.
43. Dietrich, B.; Viout, P.; Lehn, J. M. Aspects de la chimie des composés macrocycliques; Savoirs Actuels, InterEditions, Edition du CNRS, Paris: 1991; p 6.
44. Hanbook of Chemistry and Physics, 78th ed.; Lide, D. R., Ed. CRC Press: New York, 1997–1998; pp 6-173 and 6-174.
45. Delaforge, M.; André, F.; Jaouen, M.; Dolgos, H.; Benech, H.; Gomis, J. M.; Noël, J. P.; Cavelier, F.; Verducci, J.; Aubagnac, J. L.; Liebermann, B. Eur J Biochem 1997, 250, 150–157.
46. Walton, J. D.; Earle, E. D.; Stahelin, H.; Grieder, A.; Hirota, A.; Suzuki, A. Experientia 1985, 41, 348–350.
47. Shute, R. E.; Dunlap, B.; Rich, D. H. J Med Chem 1987, 30, 71–78.
48. Ludwigsen, S.; Andersen, K. V.; Poulsen, F. M. J Mol Biol 1991, 217, 731–736.
49. Wüthrich, K. NMR of Proteins and Nucleic Acids; John Wiley & Sons : New York, 1986.